Figure S4. Body Weight and Glucose Homeostasis in Wild-Type and *Eif4ebp*$^{-/-}$ Mice Fed Standard Chow or a High-Fat Diet

(A) Fed blood glucose levels of wild-type and *Eif4ebp*$^{-/-}$ mice on standard chow or a high-fat diet (HFD; Research Diets D12451).

(B) Blood glucose levels during intraperitoneal glucose tolerance tests (2 g glucose per kg of body weight) in wild-type and *Eif4ebp*$^{-/-}$ mice fed chow or a HFD at 24 weeks of age.

(C) Plasma insulin levels during intraperitoneal glucose tolerance tests (2 g glucose per kg of body weight) in wild-type and *Eif4ebp*$^{-/-}$ mice fed chow or a HFD at 26 weeks of age.

(D) Pancreatic insulin contents of wild-type and *Eif4ebp*$^{-/-}$ mice fed chow or a HFD at 28 weeks of age.

(E) Growth curves of wild-type and *Eif4ebp*$^{-/-}$ mice fed chow or a HFD.

(F) Insulin tolerance tests in wild-type and *Eif4ebp*$^{-/-}$ mice fed chow or a HFD at 25 weeks of age. After a 6 hr fast, mice were given an intraperitoneal injection of insulin (0.75 μU/g body weight). Blood glucose levels at time zero were 69 ± 5 (chow-fed wild-type), 84 ± 11 (chow-fed *Eif4ebp1*$^{-/-}$), 79 ± 5 (HFD-fed wild-type) and 107 ± 6 mg/dl (HFD-fed *Eif4ebp1*$^{-/-}$).

*$p < 0.05$ and **$p < 0.01$, between HFD-fed *Eif4ebp*$^{-/-}$ and HFD-fed wild-type mice. n = 4-6.

Error bars show SEM.

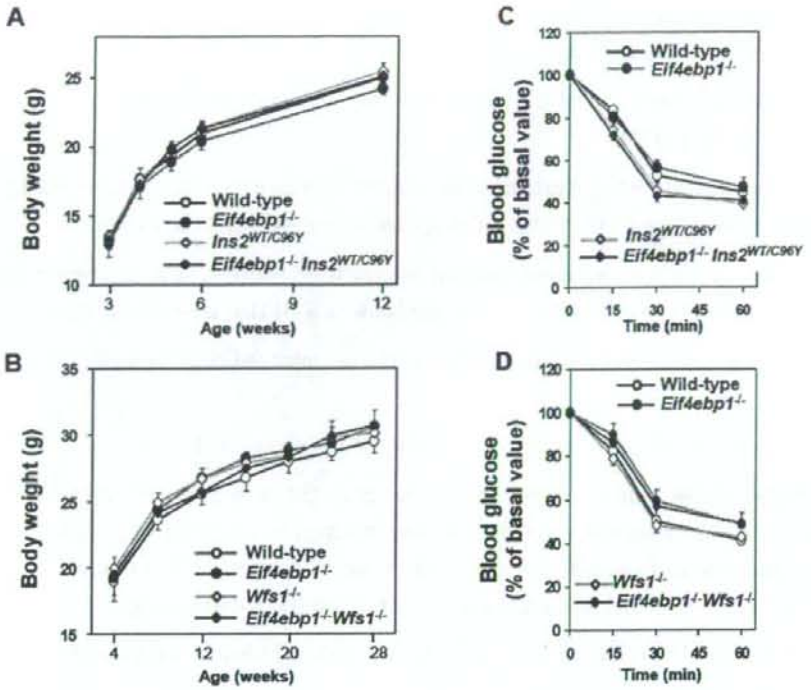

Figure S5. Characterization of 4E-BP1-Deficient *Ins2*$^{WT/C96Y}$ and *Wfs1*$^{-/-}$ Mice

(A) Growth curves of wild-type, *Eif4ebp*$^{-/-}$, *Ins2*$^{WT/C96Y}$ and *Eif4ebp1*$^{-/-}$*Ins2*$^{WT/C96Y}$ mice. n = 5-11.

(B) Growth curves of wild-type, *Eif4ebp1*$^{-/-}$, *Wfs1*$^{-/-}$ and *Eif4ebp1*$^{-/-}$*Wfs1*$^{-/-}$ mice. n = 8-15.

(C) Intraperitoneal insulin tolerance tests in wild-type, *Eif4ebp1*$^{-/-}$, *Ins2*$^{WT/C96Y}$ and *Eif4ebp1*$^{-/-}$*Ins2*$^{WT/C96Y}$ mice at 5 weeks of age. After a 6 hr fast, mice were given an intraperitoneal injection of insulin (0.75 μU/g body weight). Blood glucose levels at time zero were 77 ± 6 (wild-type), 72 ± 5 (*Eif4ebp1*$^{-/-}$), 216 ± 19 (*Ins2*$^{WT/C96Y}$) and 271 ± 23 mg/dl (*Eif4ebp1*$^{-/-}$*Ins2*$^{WT/C96Y}$). n = 5-8. Insulin sensitivities did not differ among the four groups.

(D) Insulin tolerance tests in wild-type, *Eif4ebp1*$^{-/-}$, *Wfs1*$^{-/-}$ and *Eif4ebp1*$^{-/-}$*Wfs1*$^{-/-}$ mice at 24 weeks of age. After a 6 hr fast (time zero), blood glucose was reduced to similar levels in all four groups; blood glucose levels at time zero were 79 ± 6 (wild-type), 73 ± 5 (*Eif4ebp1*$^{-/-}$), 80 ± 7 (*Wfs1*$^{-/-}$) and 77 ± 9 mg/dl (*Eif4ebp1*$^{-/-}$*Wfs1*$^{-/-}$), n = 7-9. Insulin sensitivities did not differ among the four groups ($p > 0.094$).

Error bars show SEM.

Figure S6. 4E-BP1 Protein Is Stable within Cells

MIN6 cells were incubated with thapsigargin (0.5 μM) for 24 hr, washed with PBS and treated with cycloheximide (CHX, 50 μM) for the indicated period. Cell lysates were subjected to immunoblotting with an anti-4E-BP1 antibody. Immunoblotting results for CHOP are also presented for comparison. The data are representative of three independent experiments.

Supplemental References

Lee, A.-H., Iwakoshi, N.N., and Glimcher, L.H. (2003). XBP-1 regulates a subset of endoplasmic reticulum resident chaperone genes in the unfolded protein response. Mol. Cell. Biol. 2003. *23*, 7448-7459.

Yoshida, H., Okada, T., Haze, K., Yanagi, H., Yura, T., Negishi, M., and Mori, K. (2000). ATF6 activated by proteolysis binds in the presence of NF-Y (CBF) directly to the cis-acting element responsible for the mammalian unfolded protein response. Mol. Cell. Biol. *20*, 6755-6767.

Available online at www.sciencedirect.com
ScienceDirect
Comparative Immunology, Microbiology & Infectious Diseases 31 (2008) 435–448
COMPARATIVE IMMUNOLOGY MICROBIOLOGY & INFECTIOUS DISEASES
www.elsevier.com/locate/cimid

Comparative aspects on the role of polypyrimidine tract-binding protein in internal initiation of hepatitis C virus and picornavirus RNAs

T. Nishimura[a,e], M. Saito[a], T. Takano[a,b,c], A. Nomoto[d], M. Kohara[b], K. Tsukiyama-Kohara[a,b,c,*]

[a]*Department of Experimental Phylaxiology, Faculty of Medical and Pharmaceutical Sciences, Kumamoto University 1-1-1, Honjo, Kumamoto 860-8556, Japan*
[b]*Department of Microbiology and Cell Biology, The Tokyo Metropolitan Institute of Medical Science, Tokyo 113-8613, Japan*
[c]*Laboratory Animal Research Center, Institute of Medical Science, The University of Tokyo, Tokyo 108-8639, Japan*
[d]*Graduate School of Medicine, The University of Tokyo, Tokyo 113-0033, Japan*
[e]*The Chemo-Sero-Therapeutic Research Institute, Tokyo 869-1298, Japan*

Accepted 6 July 2007

Abstract

We compared the effects of polypyrimidine tract-binding protein (PTB) on hepatitis C virus (HCV genotype IIa), encephalomyocarditis virus (EMCV) and poliovirus internal ribosome entry site (IRES) activities *in vitro*. It bound strongly to EMCV IRES, but weakly to PV and HCV RNAs. PV IRES showed the strongest dependency to PTB and it showed less than one-tenth of IRES activity after the immuno-depletion of PTB from HeLa S10 lysate with pre-coated anti-PTB IgG beads, comparing to the normal IgG beads-treated S10 lysate. EMCV IRES activity was approximately 40% of that of normal control after PTB depletion.

*Corresponding author. Department of Experimental Phylaxiology, Faculty of Medical and Pharmaceutical Sciences, Kumamoto University 1-1-1, Honjo, Kumamoto 860-8556, Japan.
Tel./fax: +81 96 373 5560.
E-mail address: kkohara@kumamoto-u.ac.jp (K. Tsukiyama-Kohara).

0147-9571/$ - see front matter
doi:10.1016/j.cimid.2007.07.002

Especially, HCV IRES activity was approximately 95%, and most weekly affected by the depletion of PTB. Repletion of PTB to depleted S10 lysate restored activities of PV and EMCV IRESs. The data suggest that PTB plays an important role in picornaviral IRESs, but not in HCV IRES.

Keywords: PTB; HCV; IRES; EMCV; PV; HeLa

Résumé

Dans notre étude, nous avons comparé les effet de la 'polypyrimidine track-binding' (PTB) virus de l'hépatite C (génotype IIa) et l'activité du virus encéphalomyodardite (EMCV) et de l'IRES du poliovirus *in vitro*. La PTB se fixe de manière résistante à l'IRES de l'EMCV mais de manière fragile à l'ARN du PV et du VHC. L'IRES du PV montre la dépendance la plus forte à la PTB et il montre une activité d'IRES de moins de un dixième après immuno-déplétion de la PTB du lysat HeLa10 par des billes d'IgG anti-PTB prêtes à l'emploi, par rapport au HeLa10 traité par des billes d'IgG normales. L'activité de l'IRES de l'EMCV était approximativement égale à 40% de celle sous contrôle normal après déplétion de la PTB. L'activité de l'IRES du VHC était approximativement égale à 95% et la moins sensible à la déplétion de la PTB. La réplétion de la PTB au lysat S10 appauvri rétablit les activités des IRES du PV et de l'EMCV. Les données suggèrent que la PTB joue un rôle important dans les IRES picornaviraux mais pas dans les IRES du VHC. De plus,

Mots clés: PTB; VHC; PTB; IRES; PV; HeLa

1. Introduction

Hepatitis C virus (HCV) possesses a single-stranded RNA (approximately 9610 nucleotides), and classified into the family *Flaviviridae* [1–4]. HCV is a major causative agent of non-A non-B hepatitis, and likely progresses into the chronic hepatitis, cirrhosis and hepatocellular carcinoma.

The 5′ untranslated region (5′UTR) of HCV RNA genome is 341 nucleotides and an internal ribosome entry site (IRES) has been proven to exist in this region [5]. Activities of IRESs of HCV were different from each genotype, and genotype IIa showed almost two-fold higher IRES activity than genotype Ib [6,7].

The IRESs have been discovered in the *Picornavirus* genomes and have a complex RNA secondary structure [5,8]. The importance of secondary structure to IRES function is understood by studies that sequence substitutions within the IRES are accompanied by compensatory mutations that act to maintain the RNA secondary structure. The 40S ribosome subunit is recruited within these IRES without binding to the m^7G cap and eIF4E [9,10]. IRESs can be classified into at least 3 groups, according to their features. IRESs derived from entero- and rhinoviruses are classified into type 1(poliovirus), and oligopyrimidine tract is located in 50–100 nucleotides past the 3′ end of the IRES [11,12]. The oligopyrimidine tract

immediately follows the 3′ end of type 2 (cardio- and aphthoviruses) IRES. Encephalomyocarditis virus (EMCV) and foot and mouse disease virus possess type 2 IRESs and utilyzes eIF4G and 4B [13,14]. The HCV and classical swine fever virus (CSFV) possess type 3 IRESs which interact directly to 40S ribosome subunit and eIF3 [15]. In addition to the requirement for eIF in each IRESs, the existence of internal initiation trans-acting factors (ITAFs) has been reported [16,17]. One of ITAFs binds to picornavirus and HCV IRES commonly is polypyrimidine tract-binding protein (PTB) [11,18–20]. PTB may work in each IRESs, however, its exact role in internal initiation has been still unclear at present. In the present study, requirement of PTB in poliovirus, EMCV and HCV IRESs has been characterized, and compared in *in vitro* translation system by depletion and complementation of PTB.

2. Materials and methods

2.1. Isolation of cDNA clones and construction of expression vectors

HCV cDNA that corresponds to nucleotide positions 1-418 (GenBank) was isolated by PCR from plasma of HCV type IIa infected patients [5], using a sense primer, 5′-GATCTAGAGCCCGCCCCCTGATGGGGGCGA-3′, and antisense primer 5′-TGTCCTGCAGTTCAAGGGCCC-3′. The amplified cDNA was digested with XbaI and AatII, and replaced with an XbaI and AatII fragment (5′UTR) of pkIV [5]. A whole cDNA which was excised by XbaI-HindIII was filled up with Klenow fragment (Takara) and cloned into StuI site of pNar3 [5], and the resulting plasmid was designated as pNII5′.

Poliovirus cDNA expression vector T7M2, CAT gene with 5′UTR of EMCV (pBSECAT) and T7CAT were constructed, as described previously [19,21].

PTB cDNA that encodes whole coding region (amino acids no. 1-531) [22] or C terminal half (amino acids no. 291-531) of PTB was synthesized by RT-PCR, and cloned into the downstream of glutathione S transferase (GST) protein in frame in pGEX-KG vector, and was designated as pGST-PTB.

2.2. Expression of PTB and production of specific antibodies

The pGST-PTB was transformed in *Esherichia coli* strain SCS-1 and induced expression with 1 mM IPTG induction. *E. coli* culture (40 ml) was peletted by centrifuge and lyzed with lysozyme (1 mg/ml) and sonicated with 1% TritonX100 and 10 mM DTT. The supernatant was reacted to Glutathione Sepharose 4B (Amersham Bioscience), cleaved by thrombin (SIGMA) and purified with ploy U Sepharose 4B (Amersham Bioscience), as described previously [22]. Rabbits or guinea pigs immunized were over four times intradermal and subcutaneously or intraperitonealy with purified recombinant whole or C-terminal half of PTB (200 μg). These hyperimmune sera were purified by the protein G Sepharose 4B (Amersham Bioscience). The anti PTB rabbit IgG was further purified by the affinity

column of PTB cross-linking Formyl Cellulofine (Seikagaku Kogyo Co.), as described by manufacturer's instruction manual.

2.3. UV cross-linking assays and immunoprecipitation

RNA probes corresponding to nucleotide(nt.) 1-341 of the HCV 5′UTR, nt. 260-833 of the EMCV 5′UTR and nt. 1-747 of the PV 5′UTR were generated by the digestion of pNII5′ with BspHI, pBSECAT with BalI and pM1(T7) with HgiAI, respectively, and transcribed by using Megascript™ T7 RNA polymerase kit (Ambion) with [α-^{32}P]UTP (NEN). Labelled RNA probes were purified by the Nuc Trap™ push columns (Stratagene). Probes ($1-5 \times 10^6$ cpm) were incubated with or without competitor RNA in HeLa S10 lysate (10 μg) at 30 °C for 20 min and irradiated on ice for 20 min in a UV Stratalinker (Stratagene). Unbound RNAs were digested with 10 μg of RNase A (Sigma), 200 units of RNase T1 (Gibco BRL) and 1 unit of phosphodiesterase I (Amersham Bioscience). Samples were analyzed by SDS-PAGE and dried gel was exposed to imaging plate (Fuji) or X-ray film (Kodak). Radioactivity was measured by the Bio-image analyzer BAS 2000 (Fuji).

HeLa S10 or recombinant PTB which was UV cross-linked to labeled HCV RNA was solubilyzed by single lysis buffer containing 1% NP40, reacted with affinity-purified anti-PTB Ig (4 μg) and precipitated by affigel protein A (Bio Rad) beads. Precipitated protein was further characterized by SDS-PAGE.

2.4. Immuno-depletion test

Affigel protein A (Bio Rad) 50 μl was pretreated with HeLa S10 100 μl at 37 °C for 1 h. The affinity purified anti-PTB Rabbit IgG (500 μg) was added, and rotated at room temperature for 3 h. These IgG beads were coated by 10% FCS-0.1 M phosphate buffer (pH 8.0) at 37 °C for 1 h, washed with S10 dialysis buffer (10 mM Hepes-KOH pH7.5, 90 mM KOAc, 1.5 mM $Mg(OAc)_2$), and reacted to HeLa S10 lysate (150 μl) at 4 °C overnight. The supernatants of each reaction were utilized for *in vitro* translation.

2.5. Competitive ELISA

Serocluster 'U' vinyl plate with 96 wells (Costar) was coated with affinity purified rabbit anti-PTB-C term IgG (2.5 μg/ml) at 4 °C overnight. After blocking with 1% casein PBS (–) at 25 °C for 2 h, non-treated or immunodepleted HeLa S10 lysate were added to each well, and incubate at 25 °C for 2 h. Purified recombinant PTB was used for standard and non-treated or immunodepleted HeLa S10 lysates were added to each well, and incubate at 25 °C for 2 h. Then anti-PTB guinea pig IgG (1 μg/ml) was reacted at 37 °C for 1 h, and finally anti-guineapig -IgG HRP (Dako 1:2000) was reacted at 37 °C for 1 h. *Ortho*-phenylene diamine was added to each well as substrate, and the absorbance was measured by microplate reader Model 450 (Bio Rad).

2.6. In vitro transcription and translation

Plasmids were linearized by digestion with XmnI (pNII5′), HpaI (pBSECAT) and NheI (p(M1)T7) and transcribed into RNA by Megascript™ T7 RNA polymerase kit (Ambion). RNAs were treated with DNase I, precipitated with LiCl, and quantitated by the Spectrophotometer DU64 (Beckman).

Synthetic RNAs (pNII5′ RNA; 1.0 pmol, pBSECAT; 1.8 pmol, p(M1)T7; 0.36 pmol and they were optimized for the linear phase in translation activity) were translated in HeLa S10 lysates at 37 °C for 30 min with [^{35}S]-Methionine (ICN), as described previously[5] . Translation products were analyzed using 7.5–15% gradient SDS-PAGE.

2.7. Restoration assay

Purified recombinant PTB, bovine serum albumin and ribosome salt wash (RSW) were dialyzed to S10 dialysis buffer, and added to PTB depleted or non-treated HeLa S10. RSW (total 6.7 ml) was prepared from 6.11 of HeLa S10, as described previously [5] (kindly supplied by Dr. H. Toyoda).

3. Results

3.1. Fifty-seven and 60 kDa doublet protein bound HCV, EMCV and PV RNA

HeLa cytoplasmic proteins that were detected by UV cross-linking to ^{32}P-UTP labeled RNA derived from the HCV, EMCV, and PV 5′UTR were compared (Fig. 1). Total counts of binding proteins in HCV RNA was five times lower than those of EMCV RNA, and three times lower than those of PV-RNA (PSL; HCV 21536.9, EMCV 105622.8, PV 59307.9). Among these cytoplasmic proteins, 57 and 60 kDa doublet bands on HCV RNA,EMCV RNA and PV RNA have been identified to be PTB (Fig. 1, indicated by asterisk). According to band intensities of the 57 and 60 kDa proteins, PTB bound to EMCV IRES most abundantly, and more diminished amount of PTB bound to PV and HCV IRESs (Fig. 1).

3.2. Identification of P57/60 kDa doublet protein on HCV-RNA as PTB

HCV-IRES-binding proteins with molecular weight of 57/60 kDa were further characterized. The recombinant PTB protein was expressed in *E. coli.* in the presence of IPTG, purified by glutathione sepharose and polyU sepharose column (Fig. 2A), and reacted with affinity purified anti-PTB IgG (Fig. 2B), as described in Section 2. Labeled HCV RNA 5′UTR was cross-linked to HeLa S10 lysate, and immunoprecipitated by affinity purified anti-PTB IgG (Fig. 3). The 57 and 60 kDa doublet bands were specifically reacted to the anti-PTB IgG (Fig. 3, lane HeLa). The recombinant PTB protein was cross-linked with HCV RNA 5′UTR and precipitated with anti-PTB IgG (Fig. 3, lane PTB). These results strongly indicate that PTB

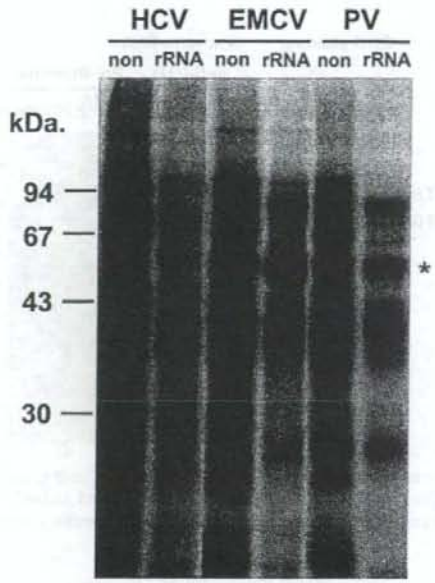

Fig. 1. UV-cross-linking analysis of binding factors to HCV, EMCV and PV-IRES RNAs. Each reaction without competitor indicates "non", and with competitor rRNA indicates rRNA on the top of the lanes. Asterisk indicates the position of PTB proteins. An asterisk indicates PTB binding.

specifically bound to HCV RNA 5′UTR, and observed as doublet protein with molecular weight of 57 and 60 kDa.

3.3. Depletion of PTB in HeLa S10 lysate

Previous results indicated the possibility that other factors than canonical eukaryotic translation initiation factors (eIFs) are working in cap independent translation. PTB is one of the candidates and when the PTB might be commonly used in several kinds of IRESs, it might play the central role in internal initiation. To compare the significance of PTB in translation initiation in HCV and other Picorna virus IRESs, PTB in HeLa S10 lysate was depleted by affinity purified anti-PTB IgG. For the depletion of PTB, pre-coating of Affi-gel protein A beads was necessary to block the non-specific adsorption, as described in Section 2. Pre-coated beads were reacted with anti-PTB IgG. From the preliminary experiments, more than 100 times higher molar ratio of anti-PTB IgG to PTB in S10 lysates was required for the over 90% depletion, as described in Materials and methods. We performed the PTB depletion, and 94.5% of PTB was depleted by anti-PTB IgG and 26.3% of PTB was depleted by pre-immune IgG (Fig. 4). We further examined the effect of PTB

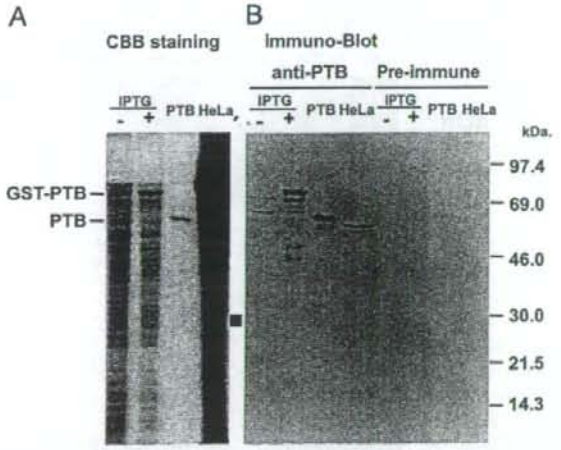

Fig. 2. Expression of recombinant PTB protein fused with GST in *E. coli*: (A) Expression of PTB protein was induced by IPTG, purified by glutathione sepharose column and stained with CBB. (B) Expressed recombinant PTB was transferred to membrane and reacted with specific antibody by WB.

depletion to the binding of cellular factors to three IRESs (Fig. 5). In PTB depleted lysates, binding of 57 and 60 kDa doublet protein was decreased, especially in PV-RNA. However, binding of other factors was not influenced significantly, other than 28 kDa protein (Fig. 5, indicated by an arrow).

3.4. Effect of PTB depletion in translation

Influence of PTB depletion was examined in HCV, EMCV and PV-RNA (Fig. 6A, Table 1). The reaction curves of each RNA were different from each other (data not shown), and the optimum quantity of each RNA used in this study was different from each other (Table 1). From the comparison of translation activity in PTB depleted S10 lysates, translation of PV-RNA was significantly decreased in 4 and 8 μl lysates (22–4.5%, 15–0.9%, Table 1, Fig. 6A). Translation of EMCV-IRES was significantly decreased after PTB depletion (53–44% (4 μl), 28–11% (8 μl)), but this suppression was not as much as PV-IRES. Activity of HCV-IRES was almost similar between pre-immune IgG-treated and anti-PTB IgG-treated S10 lysates. Because the optimal RNA quantities for translation are different in each IRESs, therefore, we calculated the ratio of PTB quantity per template RNA molecules (PTB/RNA) (ng/pmol; Table 1). In PV-IRES, translation activity was significantly reduced after depletion (4.5%, 0.9%) and the PTB/RNA ratio was 1.4 and 0.56. EMCV-IRES and HCV-IRES activity. Influence of PTB depletion to HCV-IRES activity was much lower than those of PV and EMCV.

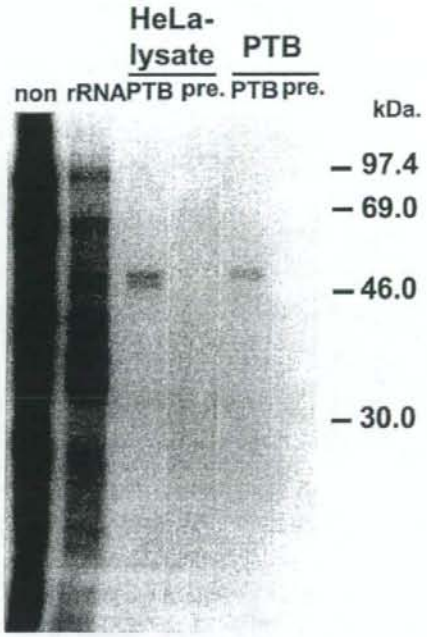

Fig. 3. HCV-IRES cross-linked S10 and PTB was immuno-precipitated by purified anti PTB antibody and pre-immune antibody. The 57 and 60 kDa doublet bands were specifically reacted to the anti-PTB IgG (lane HeLa). The recombinant PTB protein was cross-linked with HCV RNA 5′UTR and precipitated with anti-PTB IgG (lane PTB). Pre-immune antibody did not reacted to both Hela S10 and PTB.

The IRES activity of EMCV and PV-RNA was decreased by treatment of pre-immune IgG, however, treatment of pre-immune IgG did not influence significantly to the IRES activity of HCV-RNA.

3.5. Restoration of PTB to depleted S10

To clarify the effect of immuno-depletion was mainly caused by the decreased quantity of PTB, the purified recombinant PTB or RSW was added to depleted S10 (Fig. 6B). The IRES activity of PV-RNA in depleted S10 lysate (6 μl) was increased by the addition of PTB in dose-dependent manner. The EMCV-IRES activity was recovered even in the presence of 1 μg of PTB in depleted S10 lysate (4.0 μl). When too much quantity of PTB was added to the S10, translation activity of PV, EMCV and HCV decreased (over 10 times of PTB in PV, over 300 times in EMCV and over 500 times in HCV RNA, data not shown).

Translation activity of PV and EMCV-RNA became higher after the addition of RSW to anti-PTB IgG depleted S10 (150% and117%, respectively) (date not

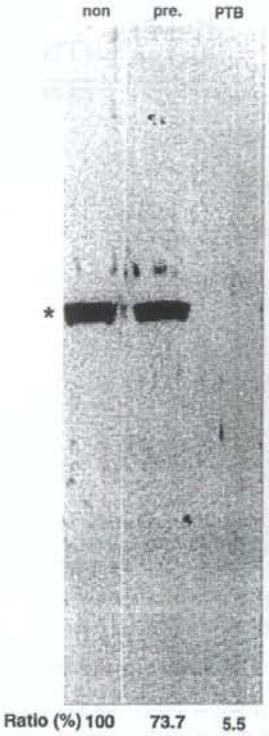

Fig. 4. Depletion of HeLa S10 by pre-immune IgG and affinity purified anti-PTB IgG. They were reacted with anti-PTB antibody by WB. Asterisk indicates the position of PTB proteins. Anti-PTB IgG deplete 94.5% of PTB (lane PTB) and pre-immune IgG deplete 26.3% of PTB (lane pre).

shown). This might indicate the existence of several translation factors other than PTB, which were lost during the treatment of IgG.

Taken together, results of this study strongly indicate that significance of PTB was highest in PV-IRES and was lowest implication in HCV-IRES.

4. Discussion

In present study, the significance of PTB in HCV, EMCV and PV IRESs has been compared. From the immuno-depletion experiment (Table 1), PTB-Ig depleted S10 (4.0 μl) contained 0.009 molecule of PTB per 1 molecule of RNA, in which PV IRES activity is 0.9%. This may indicate that almost one PTB molecule should be required

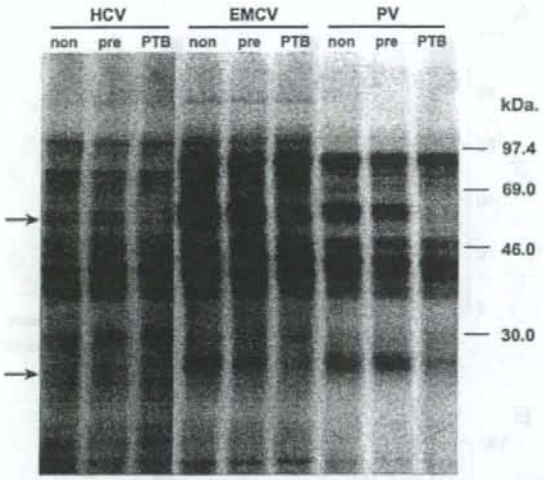

Fig. 5. UV-cross-linking analysis of HCV, EMCV and PV RNA with non-treated, pre-immune IgG-treated, and anti-PTB IgG-treated HeLa S10 lysate (lane non, pre, PTB). Upper arrow indicates the binding of PTB. Doublet protein (57 and 60 kDa) was decreased, especially in PV-RNA. Lower arrow indicates 28 kDa protein.

for 100% activity of PV IRES-RNA. In the case of EMCV IRES-RNA, 0.002 molecule of PTB per RNA gave 11% of EMCV IRES activity, and that of HCV IRES, 0.0025 molecule of PTB gave 31% of HCV IRES activity. Therefore, requirement of PTB for IRES activity was highest in PV, and less in EMCV and HCV IRES-RNA.

From the results in this study, we can compare the requirement amount of PTB in IRES activity with those of canonical eIFs. The most limiting initiation factor in cells is eIF4E, with estimates in rabbit reticulocyte lysates ranging from 0.02 copies [23] to 1 copy [24] per ribosome. The concentration of ribosomes has been estimated to be approximately 2 μM [25]. From the results of *in vitro* translation experiment, PTB should work at 0.1–0.15 M in each IRESs at maximum activity (Table 1). Therefore, working concentration of PTB for IRES activity should show almost similar to those of eIFs.

During the immuno-depletion experiment, treatment of normal IgG conjugated beads decreased the IRESs activity; 89 (6.5 μl) or 33 (3.5 μl)% in HCV IRES, 53 or 28% in EMCV IRES, and 22% or 15% in PV-IRES (Table 1). This may suggest the existence of unknown factors, which could be inactivated during the process of immuno-depletion experiment, and these effects in PV-IRES were highest among the IRESs. PV-IRES is classified into the type I [26], and the canonical eIFs with the exception of cap-binding protein eIF4E [27] and PTB [26], La [26] and 39 kDa poly(rC)-binding protein [26] are working. In EMCV IRES (type II), eIF4G was

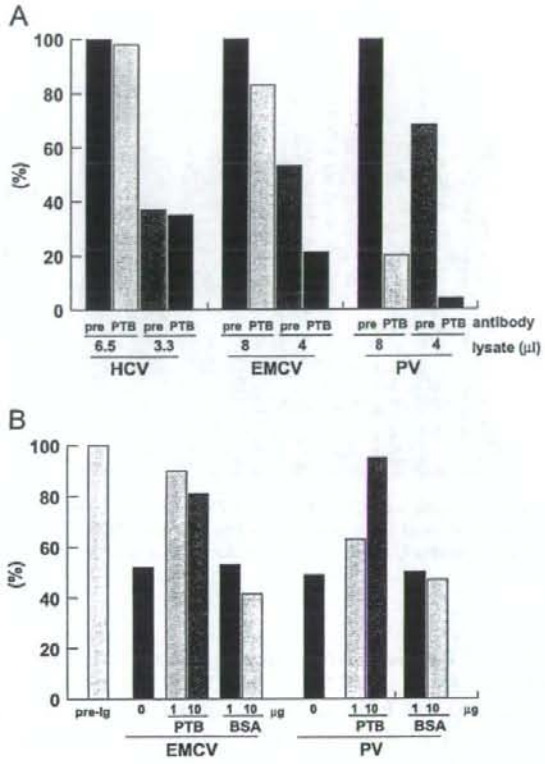

Fig. 6. (A) Effect of PTB depletion in HCV, EMCV and PV IRES. IRESs were translated in pre-immune IgG-depleted and anti-PTB IgG depleted S10 lysates (3.3, 6.5 μl in HCV-IRES, 4.0, 8.0 μl in EMCV- and PV-IRES. Translated products in SDS-PAGE were measured by image analyzer, and the quantity (PSL) of pre-immune IgG-treated S10 lysate was calculated as 100%. (B) Recovery of translation in PTB depleted S10 lysate by addition of recombinant PTB protein (1 and 10 μg. Translated products in SDS-PAGE were measured by image analyzer, and the quantity (PSL) of pre-immune IgG-treated S10 lysate was calculated as 100%.

directly bound and eIF4A and eIF4B can recruit 43S preinitiation complex which is composed of 40S ribosomal subunit and eIF3, eIF2, GTP and initiator tRNA[13]. Recent findings indicated the dependence of EMCV IRES on PTB for activity [28]. The HCV IRES possesses striking difference from type I and II IRESs, it recruits 43S preinitiation complex to initiation codon to form a 48S complex without involvement of eIF4A, 4B or 4F [29]. Thus, HCV IRES is simple and does not require most of eIFs, and might not be influenced by the depletion experiment using normal IgGs.

Table 1
Effect of PTB depletion in HCV, EMCV and PV IRES

RNA	RNA quantity (pmol)	S10 (μl)	PTB (ng)	Molar ratio of PTB to RNA	Ratio of translation (%)[a]
HCV	1.0	*Untreated*			
		6.5	7.2	0.12	100
		3.5	3.6	0.06	63
		Pre-im.-IgG			
		6.5	5.2	0.085	89
		3.5	2.6	0.045	33
		αPTB-IgG			
		6.5	0.4	0.005	87
		3.5	0.2	0.0025	31
EMCV	1.8	*Untreated*			
		8.0	8.8	0.08	100
		4.0	4.4	0.04	57
		Pre-im.-IgG			
		8.0	6.4	0.06	53
		4.0	3.2	0.03	28
		αPTB-IgG			
		8.0	0.5	0.005	44
		4.0	0.2	0.002	11
PV	0.36	*Untreated*			
		8.0	8.8	0.4	100
		4.0	4.4	0.2	65
		Pre-im.-IgG			
		8.0	6.4	0.3	22
		4.0	3.2	0.15	15
		αPTB-IgG			
		8.0	0.5	0.02	4.5
		4.0	0.2	0.009	0.9

[a]Ratio of translation products was quantitated by image analyzer.

Recent riboproteomic approach revealed the novel interacting proteins to IRESs [30], other than PTB, such as actin, forming homolog overexpressed in spleen, and microtuble interacting protein that associates with TRAF3. These factors should be characterized as novel ITAFs and comparative aspects in different IRESs should be addressed in the future work to clarify the character of each IRESs.

Acknowledgments

This work was supported by the grants from the Ministry of Health and Welfare, or Education, Culture, Sports, Science and Technology of Japan, the program for

promotion of fundamental studies in health sciences of the National Institute of Biomedical Innovation, and the Cooperative Research Project on Clinical and Epidemiological Studies of Emerging and Re-emerging Infectious Diseases.

References

[1] Choo QL, Kuo G, Weiner AJ, Overby LR, Bradley DW, Houghton M. Isolation of a cDNA clone derived from a blood-borne non-A, non-B viral hepatitis genome. Science 1989;244:359–62.
[2] Takamizawa A, Mori C, Fuke I, Manabe S, Murakami S, Fujita J, et al. Structure and organization of the hepatitis C virus genome isolated from human carriers. J Virol 1991;65:1105–13.
[3] Kato N, Hijikata M, Ootsuyama Y, Nakagawa M, Ohkoshi S, Sugimura T, et al. Molecular cloning of the human hepatitis C virus genome from Japanese patients with non-A, non-B hepatitis. Proc Natl Acad Sci USA 1990;87:9524–8.
[4] Kaito M, Watanabe S, Tsukiyama-Kohara K, Yamaguchi K, Kobayashi Y, Konishi M, et al. Hepatitis C virus particle detected by immunoelectron microscopic study. J Gen Virol 1994;75(Part 7):1755–60.
[5] Tsukiyama-Kohara K, Iizuka N, Kohara M, Nomota A. Internal ribosome entry site within hepatitis C virus RNA. J Virol 1992;66:1476–83.
[6] Kamoshita N, Tsukiyama-Kohara K, Kohara M, Nomoto A. Genetic analysis of internal ribosomal entry site on hepatitis C virus RNA: implication for involvement of the highly ordered structure and cell type-specific transacting factors. Virology 1997;233:9–18.
[7] Nomoto A, Tsukiyama-Kohara K, Kohara M. Mechanism of translation initiation on hepatitis C virus RNA. Princess Takamatsu Symp 1995;25:111–9.
[8] Pelletier J, Sonenberg N. Internal initiation of translation of eukaryotic mRNA directed by a sequence derived from poliovirus RNA. Nature 1988;334:320–5.
[9] Kieft JS, Zhou K, Jubin R, Doudna JA. Mechanism of ribosome recruitment by hepatitis C IRES RNA. RNA 2001;7:194–206.
[10] Yu Y, Ji H, Doudna JA, Leary JA. Mass spectrometric analysis of the human 40S ribosomal subunit: native and HCV IRES-bound complexes. Protein Sci 2005;14:1438–46.
[11] Hellen CU, Pestova TV, Litterst M, Wimmer E. The cellular polypeptide p57 (pyrimidine tract-binding protein) binds to multiple sites in the poliovirus 5′ nontranslated region. J Virol 1994;68:941–50.
[12] Hunt SL, Jackson RJ. Polypyrimidine-tract binding protein (PTB) is necessary, but not sufficient, for efficient internal initiation of translation of human rhinovirus-2 RNA. RNA 1999;5:344–59.
[13] Kolupaeva VG, Pestova TV, Hellen CU, Shatsky IN. Translation eukaryotic initiation factor 4G recognizes a specific structural element within the internal ribosome entry site of encephalomyocarditis virus RNA. J Biol Chem 1998;273:18599–604.
[14] Kolupaeva VG, Hellen CU, Shatsky IN. Structural analysis of the interaction of the pyrimidine tract-binding protein with the internal ribosomal entry site of encephalomyocarditis virus and foot-and-mouth disease virus RNAs. RNA 1996;2:1199–212.
[15] Sizova DV, Kolupaeva VG, Pestova TV, Shatsky IN, Hellen CU. Specific interaction of eukaryotic translation initiation factor 3 with the 5′ nontranslated regions of hepatitis C virus and classical swine fever virus RNAs. J Virol 1998;72:4775–82.
[16] Witherell GW, Wimmer E. Encephalomyocarditis virus internal ribosomal entry site RNA–protein interactions. J Virol 1994;68:3183–92.
[17] Scheper GC, Voorma HO, Thomas AA. Binding of eukaryotic initiation factor-2 and trans-acting factors to the 5′ untranslated region of encephalomyocarditis virus RNA. Biochimie 1994;76:801–9.
[18] Ali N, Siddiqui A. Interaction of polypyrimidine tract-binding protein with the 5′ noncoding region of the hepatitis C virus RNA genome and its functional requirement in internal initiation of translation. J Virol 1995;69:6367–75.
[19] Jang SK, Wimmer E. Cap-independent translation of encephalomyocarditis virus RNA: structural elements of the internal ribosomal entry site and involvement of a cellular 57-kDa RNA-binding protein. Genes Dev 1990;4:1560–72.

[20] Luz N, Beck E. Interaction of a cellular 57-kDa protein with the internal translation initiation site of foot-and-mouth disease virus. J Virol 1991;65:6486–94.
[21] Jang SK, Pestova TV, Hellen CU, Witherell GW, Wimmer E. Cap-independent translation of picornavirus RNAs: structure and function of the internal ribosomal entry site. Enzyme 1990;44:292–309.
[22] Garcia-Blanco MA, Jamison SF, Sharp PA. Identification and purification of a 62,000-Da protein that binds specifically to the polypyrimidine tract of introns. Genes Dev 1989;3:1874–86.
[23] Hiremath LS, Webb NR, Rhoads RE. Immunological detection of the messenger RNA cap-binding protein. J Biol Chem 1985;260:7843–9.
[24] Rau M, Ohlmann T, Morley SJ, Pain VM. A reevaluation of the cap-binding protein, eIF4E, as a rate-limiting factor for initiation of translation in reticulocyte lysate. J Biol Chem 1996;271:8983–90.
[25] Duncan R, Hershey JW. Identification and quantitation of levels of protein synthesis initiation factors in crude HeLa cell lysates by two-dimensional polyacrylamide gel electrophoresis. J Biol Chem 1983;258:7228–35.
[26] Flint SJ, Enquist LW, Krug RM, Racaniello VR, Skalka AM, editors. Virology. Washington, DC: ASM Press; 2000.
[27] Gingras AC, Svitkin Y, Belsham GJ, Pause A, Sonenberg N. Activation of the translational suppressor 4E-BP1 following infection with encephalomyocarditis virus and poliovirus. Proc Natl Acad Sci USA 1996;93:5578–83.
[28] Kaminski A, Jackson RJ. The polypyrimidine tract binding protein (PTB) requirement for internal initiation of translation of cardiovirus RNAs is conditional rather than absolute. RNA 1998;4:626–38.
[29] Hellen CU, Pestova TV. Translation of hepatitis C virus RNA. J Viral Hepat 1999;6:79–87.
[30] Lu H, Li W, Noble WS, Payan D, Anderson DC. Riboproteomics of the hepatitis C virus internal ribosomal entry site. J Proteome Res 2004;3:949–57.

Available online at www.sciencedirect.com

ScienceDirect

Virology 375 (2008) 321–330

VIROLOGY

www.elsevier.com/locate/yviro

Measles virus induces cell-type specific changes in gene expression

Hiroki Sato [a], Reiko Honma [b], Misako Yoneda [a], Ryuichi Miura [a], Kyoko Tsukiyama-Kohara [c], Fusako Ikeda [a], Takahiro Seki [a], Shinya Watanabe [b], Chieko Kai [a,*]

[a] *Laboratory Animal Research Center, The Institute of Medical Science, The University of Tokyo, 4-6-1 Shirokanedai, Minato-ku, Tokyo 108-8639, Japan*
[b] *Clinical Informatics, Tokyo Medical and Dental University, 1-5-45 Yushima, Bunkyo-ku, Tokyo, Japan*
[c] *Faculty of Medical and Pharmaceutical Sciences, Kumamoto University, 1-1-1 Honjo, Kumamoto City, Kumamoto, Japan*

Received 16 May 2007; returned to author for revision 13 June 2007; accepted 8 February 2008
Available online 28 March 2008

Abstract

Measles virus (MV) causes various responses including the induction of immune responses, transient immunosuppression and establishment of long-lasting immunity. To obtain a comprehensive view of the effects of MV infection on target cells, DNA microarray analyses of two different cell-types were performed. An epithelial (293SLAM; a 293 cell line stably expressing SLAM) and lymphoid (COBL-a) cell line were inoculated with purified wild-type MV. Microarray analyses revealed significant differences in the regulation of cellular gene expression between these two different cells. In 293SLAM cells, upregulation of genes involved in the antiviral response was rapidly induced; in the later stages of infection, this was followed by regulation of many genes across a broad range of functional categories. On the other hand, in COBL-a cells, only a limited set of gene expression profiles was modulated after MV infection. Since it was reported that V protein of MV inhibited the IFN signaling pathway, we performed a microarray analysis using V knockout MV to evaluate V protein's effect on cellular gene expression. The V knockout MV displayed a similar profile to that of parental MV. In particular, in COBL-a cells infected with the virus, no alteration of cellular gene expression, including IFN signaling, was observed. Furthermore, IFN signaling analyzed *in vitro* was completely suppressed by MV infection in the COBL-a cells. These results reveal that MV induces different cellular responses in a cell-type specific manner. Microarray analyses will provide us useful information about potential mechanisms of MV pathogenesis.

Keywords: Measles virus; Microarray; V protein; IFN signaling; Lymphoid cells; Epithelial cells

Introduction

During measles virus (MV) infection, the virus first enters the host via the respiratory route and replicates in tracheal and bronchial epithelial cells. The virus then enters and replicates in local lymphatic tissues and spreads through the blood to infect a variety of organs. After a latent period lasting between 10 and 14 days, patients develop symptoms, such as fever, coryza, coughing, and conjunctivitis, followed by the appearance of a characteristic rash. Immune responses have been noted to occur at almost the same time the rash fades. Recovery is accompanied by life-long immunity to reinfection. Immunosuppression, including marked lymphopenia, coincides with the appearance of immune activation and lasts for several weeks after apparent recovery (Griffin, 2001). The various pathogenic forms of measles and the different immune responses are a result of the interaction between the host and the virus. There are many *in vitro* studies on the mechanisms that trigger these reactions in MV-infected cells. For example, MV infection induces innate immune and antiviral proteins, including interferon (IFN) production in MV-infected epithelial, endothelial, and glial cells (Dhib-Jalbut and Cowan, 1993; Helin et al., 2001; Noe et al., 1999; Schneider-Schaulies et al., 1993; Vidalain et al., 2002; Yokota et al., 2004). On the other hand, some reports have demonstrated contrary results suggesting that MV does not induce the production of IFN in peripheral blood mononuclear cells (PBMC) (Naniche et al., 2000). Furthermore, recent reports have indicated that a non-structural accessory protein, the V protein, encoded within the phosphoprotein (P) gene, possesses

* Corresponding author. Fax: +81 3 5449 5379.
E-mail address: ckai@ims.u-tokyo.ac.jp (C. Kai).

0042-6822/$ - see front matter © 2008 Elsevier Inc. All rights reserved.
doi:10.1016/j.virol.2008.02.015

IFN-antagonist activity (Ohno et al., 2004; Palosaari et al., 2003; Takeuchi et al., 2003; Yokota et al., 2003). However, there are discrepancies between the various studies and the full picture remains unclear.

High-density DNA microarrays can provide a powerful approach to the profiling of the simultaneous expression of thousands of genes. Previously, Bolt et al. performed DNA microarray analysis with a limited number of human genes, approximately 3000 genes, to monitor any change in the host transcriptional profile of human PBMCs after infection with MV, and found only a few genes to be upregulated by MV infection (Bolt et al., 2002). To obtain a more comprehensive view of the overall effects of MV infection in target cells, we performed DNA microarray analysis containing more than 22,000 human genes of two different cell-types. Experiments were designed to assess gene expression patterns in human epithelial and lymphoid cells, which are the cell-types that are targeted during the pathogenesis of primary MV infection. A significant difference between these cells was observed. More recently, Zilliox et al. reported a microarray analysis of MV-infected dendritic cells and identified numerous genes that were regulated by MV (622 upregulated and 931 downregulated genes) (Zilliox et al., 2006). The profile of altered gene expression in dendritic cells was similar to that in epithelial cells in our results. Interestingly, cell-type specific modulation of the IFN signaling pathway was identified in the present study. In addition, to evaluate the effect of V protein on the modulation of host gene expression, we generated V knockout MV by employing a reverse genetics system and performed microarray analysis. The present study provides an additional comprehensive view of MV effects on different cells.

Results

Preparation of cells and virus

Experiments were designed to assess patterns of gene expression in human epithelial and lymphoid cells, which are the cell-types that are targeted during the pathogenesis of primary MV infection. First, we established a human epithelial cell line that was sensitive to wild-type MV infection. We took 293 human embryonic kidney epithelial-like cells and transfected them with the signaling lymphocytic activation molecule (SLAM) gene, a receptor for wild-type MV (Tatsuo et al., 2001). The cells were highly susceptible to MV infection and showed a large syncytium post infection (data not shown). These cells were designated 293SLAM cells. To compare transcriptional response between different cell-types after MV infection, we used a novel established human lymphoid cell line, COBL-a, which was established from a cultured umbilical cord blood cell colony (Kobune et al., 2007). COBL-a cells are a T cell lineage cell line expressing CD4 (helper-T), CD38 (immature T), CD46, and CD150 (SLAM). Cells are highly sensitive to MV infection and cause CPE post infection. In addition, a wild-type MV isolated from a blood specimen using the COBL-a cells maintained pathogenicity specific for typical acute measles against cynomolgus monkeys. The COBL-a cells are therefore ideal for virus propagation and subsequent microarray assays.

We used the HL strain (Kobune et al., 1996) as a wild-type MV. MV-HL was isolated from blood leukocytes of a patient with typical measles and induced the typical clinical signs of measles, including rashes, Koplik's spots, and transient marked leukopenia in cynomolgus and squirrel monkeys. Thus, MV-HL is considered to possess the pathogenicity of acute measles. The HL strain grew well, both in COBL-a cells and 293SLAM cells, reaching a similar maximum titer in both cells (Fig. 1). Since MV-HL is propagated on B95a cells, a marmoset B-cell line transformed with Epstein–Barr virus (EBV) (Kobune et al., 1990), it was passaged twice in 293SLAM cells that were insensitive to EBV to eliminate EBV in the MV stock solution. The obtained virus solution was inoculated onto COBL-a cells and, after 3 days, no EBV contamination was confirmed by RT-PCR using EBV specific primer pairs (Teng et al., 1996) (data not shown). To obtain the necessary quantity of MV, it was propagated largely in COBL-a cells and was then purified by ultracentrifugation.

Overview of expression microarray analysis

COBL-a cells and 293SLAM cells were inoculated with purified MV at a multiplicity of infection (MOI) of 2 to ensure that every cell was in contact with infectious viral particles. Mock and infected cells were harvested at 6, 12, and 24 h post infection and isolated poly(A+) RNAs were labeled with Cyanine 3-dUTP or Cyanine 5-dUTP. The labeled samples were hybridized on microarrays representing 22,272 human genes. Hybridization signals were processed into expression ratios as log 2 values (designated mean log ratios; see Materials and methods). The genes with mean log ratios over 1 or under −1 in at least one sample were extracted, and cluster analysis was carried out. Data from all the arrays used in this paper are available at DDBJ via CIBEX (http://www.cibex.nig.ac.jp/cibex/HTML/index.html) under accession number CBX32. Interestingly, significant differences in the regulation of cellular gene expression were observed between 293SLAM and COBL-a cells (Fig. 2). The number of genes that were up- and downregulated with a mean log ratio over 1 or under −1 in individual samples is shown in Fig. 2B. In 293SLAM cells,

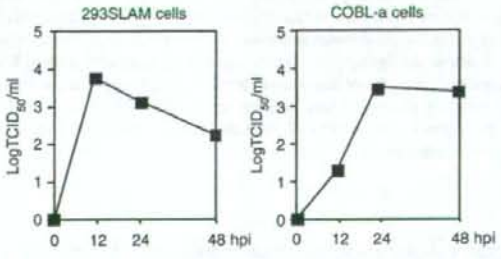

Fig. 1. Comparison of the replication of MV-HL in 293SLAM and COBL-a cells. After infection at an MOI of 0.001, the viral titer was determined by $TCID_{50}$ at the indicated time points. The average of two independent measurements is shown.

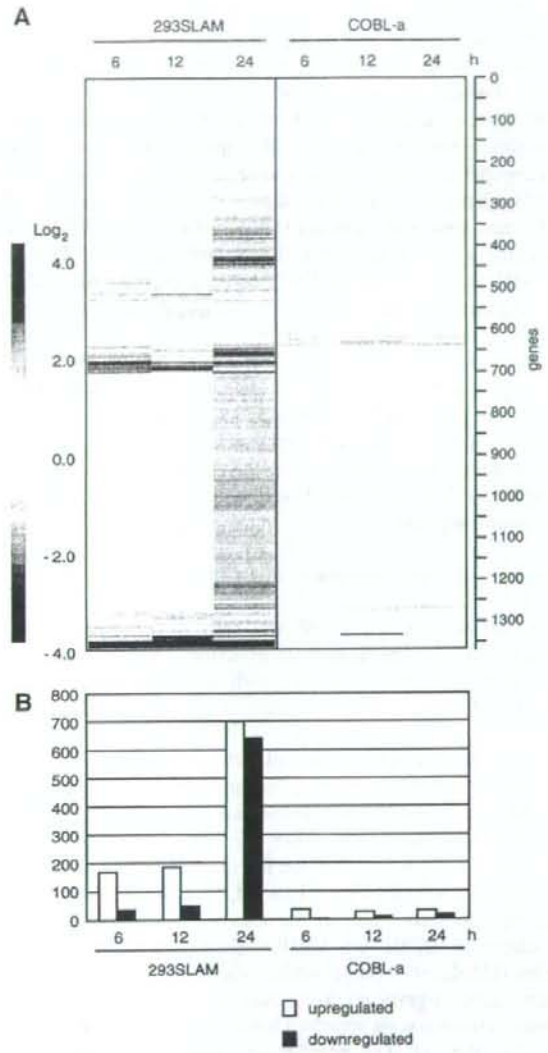

Fig. 2. Gene expression profiles of 293SLAM cells and COBL-a cells inoculated with MV-HL. (A) Genes exhibiting the mean log ratio in all 6 samples were extracted (19,415 genes). These genes were further extracted with |mean log ratio| ≥ 1, and the resulting 1,368 genes were assembled in the order obtained from the results of hierarchical clustering analysis. The y-axis of the dendrogram depicts Euclid square distance as the dissimilarity coefficient. The color bar on the left side of the figure shows expression ratio against mock-infected RNA in $\log_2$; red and blue indicate increase and decrease of mean log ratios, respectively. (B) Kinetics of changes in total gene expression after MV infection. Individual values for genes upregulated and genes downregulated by MV infection were represented graphically.

marked cellular responses were induced by MV infection, and the number of regulated genes increased over time. On the other hand, COBL-a cells showed little alteration in gene expression despite similar viral replication rates as those observed in 293SLAM cells.

Effects of MV on gene expression in 293SLAM cells

In 293SLAM cells, a series of cellular genes was found to be upregulated and downregulated by virus infection. Among genes that were altered early (6 h post infection), the most apparent characteristic was the upregulation of a series of genes that are related to innate immune and antiviral responses. This result clearly showed typical early events after virus infection, such as activation of IRF-3 and NF-kB, which result in the induction of type I IFN. Furthermore, a series of IFN signal transductions was subsequently observed. In particular, the three principal families of IFN-inducible genes (RNA-activated protein kinase [PKR], the 2′5′-oligoadenylate synthetases [OAS], and the Mx proteins) were markedly induced. In addition, activation of a broad range of functional responses that are involved in the host antiviral response, including many IFN-stimulated genes (ISG), inflammatory cytokines, and immune pathways, was demonstrated. These results show that MV infection and replication trigger a rapid and strong innate antiviral response in 293SLAM cells. The number of upregulated genes was slightly increased 12 h post infection (Fig. 2B).

At 24 h post infection, the number of upregulated genes increased significantly; 701 upregulated genes were identified. To facilitate the analysis of our data, we grouped the regulated genes according to biological functions (Table 1). Upregulation

Table 1
Classes of genes upregulated at 24 h post MV infection in 293SLAM cells

Functional classification	Number
Antivirus	60
Metabolism	31
Transcription factor, transcription regulation	30
Zinc finger protein	24
Protein kinases and phosphatases	21
Channels and transporters	18
Nucleus and nuclear matrix	16
Histocompatibility and cell surface markers	15
Oncogenesis	13
Cytoskeleton and cell structure, motor protein	13
Protein degradation	9
Apoptosis, antiapoptosis	9
Cellular development and differentiation, physiology	8
Growth factor	8
RNA processing and binding modification	8
Cell adhesion and intercellular junction, extracellular matrix	7
Cell cycle related	7
Stress response/cell defense	6
Receptor and receptor-associated	6
tRNA	6
DNA modification and replication	5
Vesicular protein trafficking and fusion, vesicular formation	5
Immunity	4
Intracellular transporter	4
Signaling	3
Hormone related	3
Homeostasis	3
Protein modification	1
Translation	1
Unknown function	49
Hypothetical protein	308
Total	701